Nonlinear MPC Based Coordinated Control of Towed Debris Using Tethered Space Robot

Bingheng Wang[1,2], Zhongjie Meng[1,2], and Panfeng Huang[1,2](✉)

[1] Research Center for Intelligent Robotics, School of Astronautics, Northwestern Polytechnical University, Xi'an 710072, Shaanxi, People's Republic of China
pfhuang@nwpu.edu.cn

[2] National Key Laboratory of Aerospace Flight Dynamics, Northwestern Polytechnical University, Xi'an 710072, Shaanxi, People's Republic of China

Abstract. Using tethered space robot (TSR) for active debris removal (ADR) is promising but subject to collision and entanglement due to the debris tumbling. To detumble the towed debris, this paper proposes the nonlinear model predictive control (NMPC) based coordinated control strategy. The TSR consists of a gripper for capture, thrusters and a tethered manipulator (TM) with variable length to which the tether is attached. The proposed strategy works in the way that the TM coordinates with the thrusters for de-tumbling by changing its length accordingly so that the tension torque can be adjusted. The attitude model of the debris is first established, followed by the definition of attitude equilibrium. The NMPC is then designed with the prediction model discretized by 4-order Runge-Kutta method. Simulation results validate this strategy and show that the debris attitude can maneuver to the equilibrium smoothly in the presence of the constraints on TM and thrusts.

Keywords: Active debris removal · Tethered space robot · Model predictive control

1 Introduction

To reduce the debris population, the use of space tether for active debris removal (ADR) proves to be promising compared to the rigid manipulator and has attracted a great deal of research interests [1–3]. This technology, also termed as 'towing removal', is achieved by employing an active maneuverable platform, attaching the tether to the debris and towing it to the disposal orbit.

However, the towing removal involves two main technical challenges, namely collision between the two end bodies and the entanglement with tether. They are mainly attributable to the flexible structure of tether and the debris tumbling [4]. Further, many factors can actually cause debris to tumble, such as residual angular velocities, off-centered capture [5] and flexible appendages [6].

Y. Huang et al. (Eds.): ICIRA 2017, Part III, LNAI 10464, pp. 698–706, 2017.
DOI: 10.1007/978-3-319-65298-6_62

As a result, debris de-tumbling is imperative for towing mission success. Taking advantages of the torque generated by the tether tension is effective and economic for de-tumbling the tethered debris, but the tether fails to yield the tension torque along itself. To achieve 3-axis detumbling, the coordinated control was proposed by Huang, et al. [7,8] which combines the varying tension with the gripper thrusters.

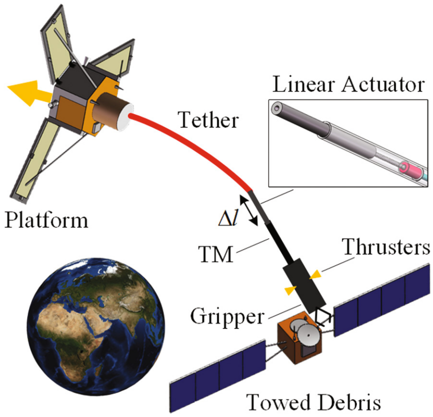

Fig. 1. Illustration of towing removal and TSR

In this paper, the coordinated control is applied to the towed debris de-tumbling. For towing removal, the tether tension should be stabilized to make debris keep pace with the platform for collision avoidance. For this respect, moving tether attachment point (TAP) is the only way to obtain the desired tension torque. Thus, the tethered space robot (TSR) is proposed that consists of a gripper for capture, thrusters and a tethered manipulator (TM), as shown in Fig. 1. The TM is a linear actuator with variable length Δl to which the tether is attached. During de-tumbling, the TM coordinates with thrusters by changing the length so that the tension torque acting on debris is adjusted.

However, the limits on thrusts and TM length change as well as the velocity of TAP pose severe challenges on controller design. Fortunately, nonlinear model predictive control (NMPC) which features feedback control and receding horizon enables the control systems to perform well in the presence of control constraints. And its many successful applications to aerospace has demonstrated the great effectiveness [9–11]. For this reason, the main contribution of this paper is to apply NMPC to the coordinated control of towed debris using TSR.

The paper is organized as follows. In Sect. 2, the attitude model of debris towed with off-centered capture by TSR is developed and the attitude equilibrium is defined. The design procedure of NMPC is presented in Sect. 3. Section 4 gives the simulation results and discussions. The conclusion is presented in Sect. 5.

2 Attitude Model and Equilibrium Definition

In this section, the attitude model of towed debris is first derived taking into account the tension torque provided by TM, then the attitude equilibrium to be tracked during detumbling is defined.

2.1 Attitude Model

The detumbling scenario begins with the debris already tethered by the off-centered capture on the bracket of solar panel using TSR. Prior to the modelling, several assumptions are made as follows.

1. The TSR is assumed to capture the debris tightly so that the relative movement between TSR and debris is negligible.
2. The debris is viewed as a rigid body.
3. The mass of TSR is negligible compared to the debris.

The attitude described by Modified Rodrigues Parameters (MRPs) is defined between the body frame of debris and local vertical local horizontal (LVLH) frame. The tension torque acting on the debris and the orientation of TSR after capture are illustrated in Fig. 2.

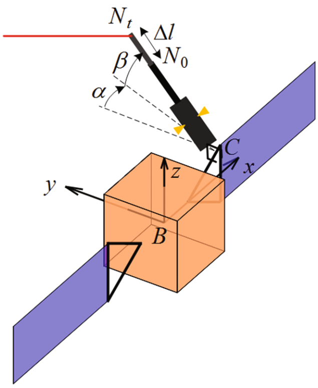

Fig. 2. Illustration of tension torque and orientation of TSR

In Fig. 2, B is the debris center of mass (CoM), C is the off-centered capture point, N_0 denotes the initial TAP when $\Delta l = 0$ and N_t represents the TAP during detumbling. The α and β are the orientation angles of TSR, according to assumption 1, they are constant when the capture is complete. As shown in Fig. 2, the tension torque $\boldsymbol{\tau}_{\mathrm{T}}$ includes two parts, namely the induced torque $\boldsymbol{\tau}_{\mathrm{T}i}$ caused by the off-centered arm $\overrightarrow{BN_0}$ and the control torque $\boldsymbol{\tau}_{\mathrm{T}c}$ caused by the length change $\overrightarrow{\Delta l}$.

$$\begin{aligned} \boldsymbol{\tau}_{\mathrm{T}} &= \boldsymbol{\tau}_{\mathrm{T}i} + \boldsymbol{\tau}_{\mathrm{T}c} \\ &= \left(\overrightarrow{BN_0} + \overrightarrow{\Delta l}\right) \times \boldsymbol{T}|_D \end{aligned} \tag{1}$$

where $\overrightarrow{\Delta l} = [\Delta l \cos\beta \sin\alpha, \Delta l \cos\beta \cos\alpha, \Delta l \sin\beta]^T$ is length change vector in body frame, $\boldsymbol{T}|_D = \boldsymbol{RT}$ is tension vector in body frame, $\boldsymbol{R}$ denotes the transformation matrix and $\boldsymbol{T}$ is tension vector in LVLH frame. Therefore, we can obtain the attitude model of the form.

$$\begin{cases} \dot{\boldsymbol{\sigma}} = \boldsymbol{G}(\boldsymbol{\sigma})\,\boldsymbol{\omega} \\ \boldsymbol{J}\dot{\boldsymbol{\omega}} = -\boldsymbol{\omega}^{\times}\boldsymbol{J}\boldsymbol{\omega} + \boldsymbol{\tau}_{\mathrm{T}} + \boldsymbol{\tau}_{\mathrm{F}} \end{cases} \tag{2}$$

where $\boldsymbol{\sigma} = [\sigma_x, \sigma_y, \sigma_z]^T \in \Re^3$ is MRPs of debris attitude, $\boldsymbol{\omega} = [\boldsymbol{\omega}_x, \boldsymbol{\omega}_y, \boldsymbol{\omega}_z]^T \in \Re^3$ is debris angular velocity. $(\cdot)^{\times} \in \Re^{3\times3}$ is a skew-symmetric operator, $\boldsymbol{J} \in \Re^{3\times3}$ is principal inertia tensor of the debris, $\boldsymbol{\tau}_F \in \Re^3$ is thruster torque, and $\boldsymbol{G}(\boldsymbol{\sigma}) = 1/4\left[\left(1 - \boldsymbol{\sigma}^T\boldsymbol{\sigma}\right)I_3 + 2\boldsymbol{\sigma}^{\times} + 2\boldsymbol{\sigma}\boldsymbol{\sigma}^T\right]$. The transformation matrix used in Eq. 1 is defined as $\boldsymbol{R}(\boldsymbol{\sigma}) \triangleq \boldsymbol{I}_3 - \frac{4\left(1-\boldsymbol{\sigma}^2\right)}{(1+\boldsymbol{\sigma}^2)^2}[\boldsymbol{\sigma}^{\times}] + \frac{8}{(1+\boldsymbol{\sigma}^2)^2}[\boldsymbol{\sigma}^{\times}]^2$.

2.2 Equilibrium Definition

The control objective is to steer the debris towards the equilibrium where the tension force acts through the debris CoM so that the attitude in this case can be stable and maintained. The equilibrium is determined by the TM length and we define that the length returns to its initial value l_0 after detumbling. As a result, the equilibrium can be obtained by the following equation.

$$\overrightarrow{BN_0} \times \boldsymbol{R}(\boldsymbol{\sigma}_{\mathrm{eq}})\,\boldsymbol{T} = 0 \tag{3}$$

where $\boldsymbol{\sigma}_{\mathrm{eq}}$ is the MRPs in equilibrium.

3 Nonlinear MPC Design

As a effective feedback optimal control, the NMPC can optimize a control sequence over a future horizon using the prediction model in order to minimize a cost function subject to constraints [9]. The first elements of the optimized control is applied to the plant over the first sampling interval. And the optimization horizon subsequently recedes and the process is repeated again. In this paper, the application of NMPC is shown in Fig. 3 where the thruster torque $\boldsymbol{\tau}_F$ and TM length change Δl are the control variables to be optimized, the errors of MRPs and angular velocity ($\boldsymbol{\sigma}_e$ and $\boldsymbol{\omega}_e$) are the state $\boldsymbol{x}$ to be controlled.

Note that the navigation system is outside the scope of this paper. Therefore, the error attitude model is first derived from Eq. 2 and then is discretized by 4-order Runge-Kutta method. The next step is to design the cost function,and the system constraints should be considered and implemented in controller.

3.1 Error Model and Discretization

Define $\boldsymbol{\sigma}_e = [\sigma_{ex}, \sigma_{ey}, \sigma_{ez}]^T$ and $\boldsymbol{\omega}_e = [\omega_{ex}, \omega_{ey}, \omega_{ez}]^T$ as:

$$\begin{cases} \boldsymbol{\sigma}_e = \boldsymbol{\sigma} \otimes \boldsymbol{\sigma}_{\mathrm{eq}}^{-1} \\ \boldsymbol{\omega}_e = \boldsymbol{\omega} - \boldsymbol{R}(\boldsymbol{\sigma}_e)\,\boldsymbol{\omega}_{\mathrm{d}} \end{cases} \tag{4}$$

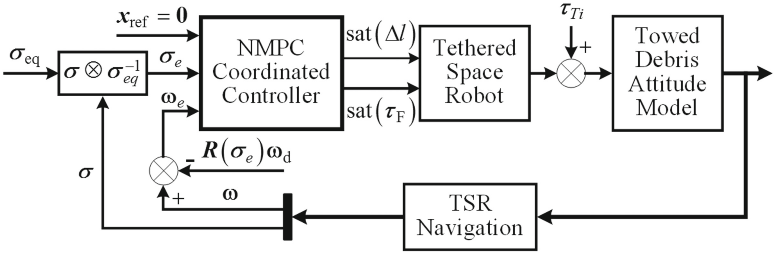

Fig. 3. The structure of NMPC coordinated controller

where $\boldsymbol{\omega}_{\text{d}}$ is the desired angular velocity and set to be zeros, The operator $\otimes$ denotes the MRP multiplication defined as below.

$$\boldsymbol{\sigma} \otimes \boldsymbol{\sigma}_{\text{eq}}^{-1} = \frac{\left(1 - \boldsymbol{\sigma}_{\text{eq}}^T \boldsymbol{\sigma}_{\text{eq}}\right) \boldsymbol{\sigma} + \left(\boldsymbol{\sigma}^T \boldsymbol{\sigma} - 1\right) \boldsymbol{\sigma}_{\text{eq}} - 2\boldsymbol{\sigma}_{\text{eq}} \times \boldsymbol{\sigma}}{1 + \left(\boldsymbol{\sigma}_{\text{eq}}^T \boldsymbol{\sigma}_{\text{eq}}\right) \left(\boldsymbol{\sigma}^T \boldsymbol{\sigma}\right) + 2\boldsymbol{\sigma}_{\text{eq}}^T \boldsymbol{\sigma}} \tag{5}$$

Therefore, the error model with the new states $\boldsymbol{x}$ can be formed as:

$$\dot{\boldsymbol{x}} = \boldsymbol{f}\left(\boldsymbol{x}, \Delta l, \boldsymbol{\tau}_{\text{F}}\right) \tag{6}$$

where $\boldsymbol{x} = \left[\boldsymbol{\sigma}_e, \boldsymbol{\omega}_e\right]^T$ and $\boldsymbol{f} = \left[\boldsymbol{G}\left(\boldsymbol{\sigma}_e\right) \boldsymbol{\omega}_e, -\boldsymbol{J}^{-1} \boldsymbol{\omega}_e{}^{\times} \boldsymbol{J} \boldsymbol{\omega}_e + \boldsymbol{J}^{-1}\left(\boldsymbol{\tau}_{\text{T}} + \boldsymbol{\tau}_{\text{F}}\right)\right]^T$.

The above continuous-time error model is discretized using the 4-order Runge-Kutta method of the form.

$$\boldsymbol{x}\left(n+1\right) = \boldsymbol{x}\left(n\right) + \frac{1}{6}\left(k_1 + 2k_2 + 2k_3 + k_4\right) \tag{7}$$

where $\boldsymbol{x}\left(n\right)$ denotes the state $\boldsymbol{x}$ at n moment and k_1, k_2, k_3, k_4 are defined as:

$$\begin{cases} k_1 = \Delta t_s f\left(\boldsymbol{x}\left(n\right), \Delta l\left(n\right), \boldsymbol{\tau}_{\text{F}}\left(n\right)\right) \\ k_2 = \Delta t_s f\left(\boldsymbol{x}\left(n\right) + 0.5k_1, \Delta l\left(n\right), \boldsymbol{\tau}_{\text{F}}\left(n\right)\right) \\ k_3 = \Delta t_s f\left(\boldsymbol{x}\left(n\right) + 0.5k_2, \Delta l\left(n\right), \boldsymbol{\tau}_{\text{F}}\left(n\right)\right) \\ k_4 = \Delta t_s f\left(\boldsymbol{x}\left(n\right) + k_3, \Delta l\left(n\right), \boldsymbol{\tau}_{\text{F}}\left(n\right)\right) \end{cases} \tag{8}$$

where $\Delta t_s = \frac{\Delta T}{m}$ is the step size, ΔT is the MPC sampling time and m is the discretization number.

3.2 Cost Function and Constraints

The cost function should be designed to penalize the state $\boldsymbol{x}$ in order to make the attitude track the equilibrium. The increments of control variables should also be penalized as the velocity of length change $\dot{\Delta l}$ is limited and a stead control is of significance. The terminal cost function F_t and constraints Ω_t are absent due to two reasons [12]. First, designing F_t and Ω_t to achieve a asymptotical stability is still an open problem. Second, including F_t and Ω_t will give rise to nonconvex optimization problems. As a result, the cost function is defined as below.

$$\overline{J}\left(\boldsymbol{x}, \Delta l, \boldsymbol{\tau}_{\mathrm{F}}\right) = \sum_{n=0}^{N-1}\left(\boldsymbol{x}(n)^{T}\boldsymbol{Q}\boldsymbol{x}\left(n\right) + \widehat{\Delta l}\left(n\right) R_{l}\widehat{\Delta l}\left(n\right) + \widehat{\boldsymbol{\tau}_{\mathrm{F}}}(n)^{T}\boldsymbol{R}_{\tau}\widehat{\boldsymbol{\tau}_{\mathrm{F}}}\left(n\right)\right) \quad (9)$$

where N is the optimization horizon, $\boldsymbol{Q}$, R_l and $\boldsymbol{R}_\tau$ are appropriate weighting matrices, and $\widehat{\Delta l}\left(n\right)$ and $\widehat{\boldsymbol{\tau}_{\mathrm{F}}}\left(n\right)$ denote the control increments.

The system constraints on states and control variables are defined as follows.

$$\begin{cases} 0 \le \Delta l\left(n\right) \le \Delta l_{\max} \\ \boldsymbol{\tau}_{\mathrm{F\,min}} \le \boldsymbol{\tau}_{\mathrm{F}}\left(n\right) \le \boldsymbol{\tau}_{\mathrm{F\,max}} \\ \boldsymbol{x}\left(0\right) = \boldsymbol{x}\left(t\right) \\ \boldsymbol{x}\left(N\right) = \boldsymbol{0} \end{cases} \quad (10)$$

where $\Delta l_{\max}$, $\boldsymbol{\tau}_{\mathrm{F\,min}}$ and $\boldsymbol{\tau}_{\mathrm{F\,max}}$ are the bounds of control variables, and $\boldsymbol{x}\left(t\right)$ is the current state.

4 Simulation and Discussion

The simulation begins with the debris already captured by TSR and being towed on the way to the disposal orbit. The inertia parameters of debris and the geometrical size of TSR are set as $\boldsymbol{J} = diag\left(1500, 2000, 3000\right)\,\mathrm{kgm}^2$ and $\left\|\overrightarrow{CN_0}\right\| = 1.7\,\mathrm{m}$. The coordinate of capture point C in body frame is defined as $C = \left[2, 0, 0.577\right]^T$. The tension vector $\boldsymbol{T}$ in LVLH frame is assumed to be constant as $\boldsymbol{T} = \left[0, 75, 0\right]^T N$. In this case, according to Eq. 3, the equilibrium is

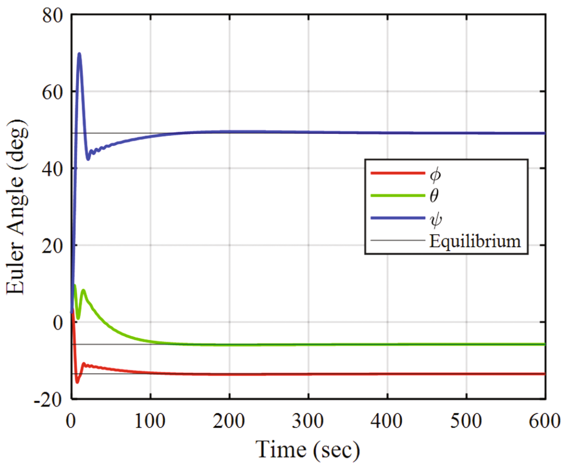

Fig. 4. Euler angles of debris

therefore obtained and can be expressed using Euler angles with 1-2-3 rotation sequence as $[\phi_{\mathrm{eq}}, \theta_{\mathrm{eq}}, \psi_{\mathrm{eq}}] = [-13.48, -5.78, 49.11]^T$ deg.

The bounds of TM length change and thruster torque are set as 1m and ± 15 Nm respectively. The ΔT is 0.1 s, m is 5 and N is 2. The state weighting matrix is $\boldsymbol{Q} = diag\left(1.2 \times 10^4, 1.5 \times 10^4, 1 \times 10^4, 2500, 2500, 2500\right)$ and weighting matrices for control are chosen as $R_l = 5$ and $\boldsymbol{R}_\tau = diag\,(0.001, 0.001, 0.001)$ respectively since the aggressive control of thruster is feasible but the quick change of the TM length should be avoided.

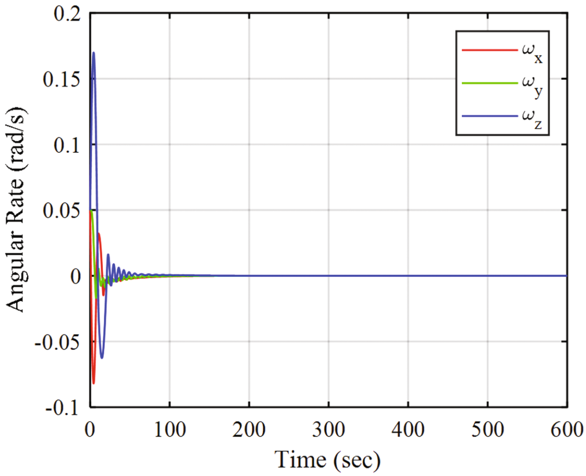

Fig. 5. Angular velocity of debris

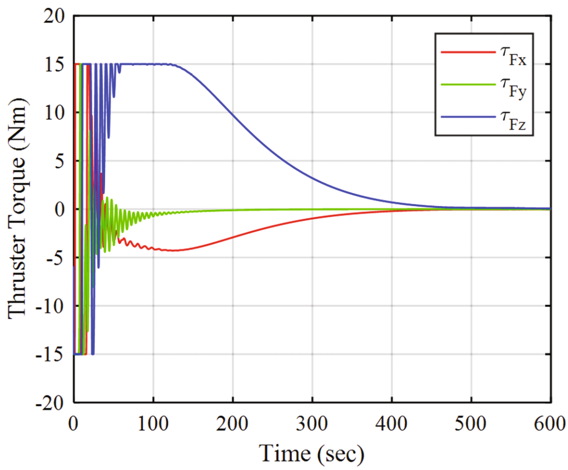

Fig. 6. Thruster control torque

Figure 4 shows that the attitude varies dramatically during the first 20 s then converge to the equilibrium smoothly. In Fig. 5, the angular velocity present the dumping oscillations and gradually decay to zeros, demonstrating the system is asymptotically stable. Figure 6 shows that the thruster torque components fluctuate within the bounds initially and begin to converge towards zeros after 120 s. Figure 7 presents the TM length change whose velocity is feasible thanks to the large weighting parameter. In Fig. 8, the total tension torque can converge to zero as the debris attitude maneuvers to the equilibrium, validating the equilibrium definition and the effectiveness of the proposed control strategy.

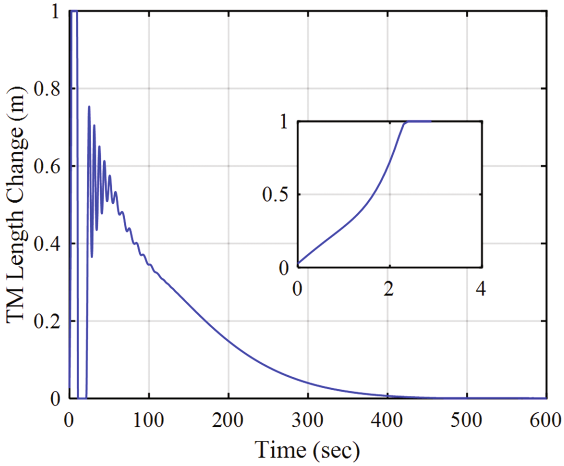

Fig. 7. TM length change

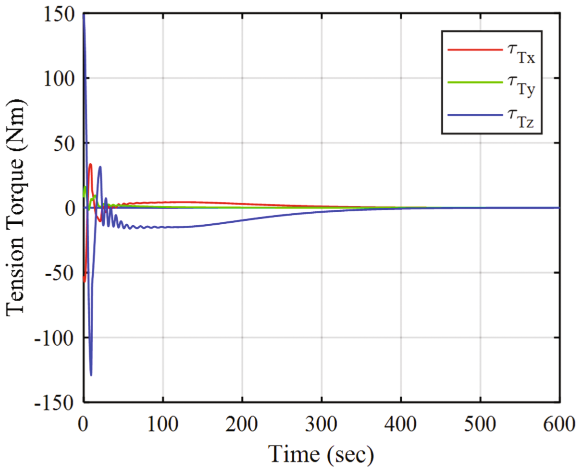

Fig. 8. The tension torque

5 Conclusion

The NMPC based coordinated control of towed debris using tethered space robot is studied in this paper. Simulation results illustrate that the TSR with the proposed control algorithm enables the debris to reorient to the equilibrium. This result is encouraging since it ensures the avoidance of the collision and entanglement, which is of significance for the safe conduction of ADR mission. In the future, a more novel TSR that uses tether only to implement detumbling control is worth discussion, and the robustness to dynamics uncertainty should be considered in controller design.

References

1. Huang, P.F., Zhang, F., Meng, Z.J.: Adaptive control for space debris removal with uncertain kinematics, dynamics and states. Acta Astro. **128**, 416–430 (2016)
2. Aslanov, V.S., Yudintsev, V.V.: Dynamics of large space debris removal using tethered space tug. Acta Astro. **91**, 149–156 (2013)
3. Qi, R., Misra, A.K., Zuo, Z.Y.: Active debris removal using double-tethered space-tug system. J. Guid. Control Dyn. **40**(3), 720–728 (2017)
4. Hovell, K., Ulrich, S.: Attitude stabilization of an uncooperative spacecraft in an orbital environment using visco-elastic tethers. In: AIAA Guidance, Navigation, and Control Conference, pp. 1–16. AIAA press, San Diego (2016)
5. Jasper, L.E.Z.: Open-loop thrust profile development for tethered towing of large space objects. Ph.D. Thesis, University of Colorado, Boulder (2014)
6. Aslanov, V.S., Yudintsev, V.V.: Behavior of tethered debris with flexible appendages. Acta Astro. **104**(1), 91–98 (2014)
7. Huang, P.F., Wang, D.K., Meng, Z.J.: Post-capture attitude control for a tethered space robot-target combination system. Robotica **33**(4), 898–919 (2015)
8. Huang, P.F., Wang, D.K., Meng, Z.J.: Adaptive postcapture backstepping control for tumbling tethered space robot target combination. J. Guid. Control Dyn. **39**(1), 150–156 (2015)
9. Petersen, C.D., Leve, F., Kolmanovsky, I.: Model predictive control of an Underactuated spacecraft with two reaction wheels. J. Guid. Control Dyn. **40**(2), 320–332 (2016)
10. Slegers, N., Kyle, J., Costello, M.: Nonlinear model predictive control technique for unmanned air vehicles. J. Guid. Control Dyn. **29**(5), 1179–1188 (2006)
11. Li, H.P., Yan, W.S., Shi, Y.: Continuous-time model predictive control of under-actuated spacecraft with bounded control torques. Automatica **75**, 144–153 (2017)
12. Yan, Z., Wang, J.: Model predictive control for tracking of underactuated vessels based on recurrent neural networks. IEEE J. Oceanic Eng. **37**(4), 717–726 (2012)